# Integrated microRNA-mRNA analyses of distinct expression profiles in hyperoxia-induced bronchopulmonary dysplasia in neonatal mice.

zhiqiang wang[1], sheng zhang[2], lina zhu[2], jun duan[3], bo huang[1], and Xiaoying Zhang[1]

[1]Guilin Medical University
[2]Bayi Children's Hospital
[3]First Affiliated Hospital of Anhui Medical University

September 11, 2020

**Abstract**

Bronchopulmonary dysplasia (BPD) is a common chronic lung disease of preterm neonates; the underlying pathogenesis is not fully understood. Recent studies suggested microRNAs (miRNAs) may be involved in BPD. In the present study, we performed miRNA and mRNA microarrays to analyze the expression profiles of miRNA and mRNA in BPD and control lung tissues. Our results showed that a total of 192 differentially expressed miRNAs (74 downregulated and 118 upregulated) and 1225 differentially expressed mRNAs (479 downregulated and 746 upregulated) were identified between BPD mice and normoxia-control mice. Bioinformatics methods including Gene Ontology (GO) and Kyoto Encyclopedia of Genes and Genomes (KEGG) were performed to predict the potential functions of differentially expressed genes. For downregulated genes, the top significant enriched GO terms and KEGG pathways were both mainly related to immune and inflammation processes. For upregulated genes, the top significant enriched GO terms and KEGG pathways were both mainly related to ECM remodeling. Quantitative Reverse Transcription-PCR, protein-protein interaction (PPI) network and miRNA-mRNA regulatory network construction were further performed to analyze the key genes and pathways associated with inflammation and immune regulation. Our findings may provide novel insights into the development of new promising biomarkers for the treatment of BPD.

## 1. INTRODUCTION

Bronchopulmonary dysplasia (BPD) is a common chronic lung disease in infants born prematurely.[1,2] Although the underlying pathogenesis is not fully understood, pulmonary inflammation is now considered to be the common signal pathway in lung and the main clinicopathological characteristic in BPD.[3,4]

MicroRNAs (miRNAs), small non-coding RNAs, which are involved in various biological processes, including tumorigenesis, inflammation, and immune regulation.[1,5,6]. Using newborn mouse models, we previously demonstrated that miRNAs are associated with lung development and that altered miRNA levels contribute to the development of BPD.[1]

With the development of gene expression profiles, comparisons of differentially expressed mRNAs or miRNAs have been carried out in many diseases including BPD.[1,7-9] Although microarray technologies are convenient, most studies focus on a single cohort study, and different studies report contrasting results. Integrated advanced bioinformatics methods may offer a way to overcome these disadvantages and elucidate the molecular mechanism involved in BPD.

In the present study, we used mRNA and miRNA microarrays to assess differential expression profiles in BPD and control lung tissues.

Bioinformatics methods including Gene Ontology (GO) and KEGG (Kyoto Encyclopedia of Genes and Genomes) pathway analyses for differentially expressed genes, and protein-protein interaction (PPI) network

and miRNA-mRNA regulatory network construction were performed to analyze the key genes and pathways associated with inflammation and immune regulation. These data would provide novel insights into the development of new promising biomarkers for the treatment of BPD.

### 2.1 Animal model

The experimental BPD mouse model was induced as we previously described.[1] Briefly, newborn Kunming mice (the Chinese Academy of Sciences Beijing, China) were randomly assigned to room air and oxygen exposure ($FiO_2$= 60% for 21days) beginning at birth (n=15 each group).[1] Animals were euthanized with intraperitoneal sodium pentobarbital after exposure on postnatal day 2 (P2), P7, and P21(n=5 each) and lung tissues were stored in liquid nitrogen.[1] All experiments involving animals were approved by the Animal Care and Use Committee of The General Military Hospital of Beijing PLA, Beijing, China.

### 2.2 Tissue collection and microarray analysis

Total RNA was isolated from individual whole lungs (P21) using miRVana kits (Ambion) according to the manufacturer's instructions and our previous report.[1] RNA quality was controlled by screening for OD 260/280 ratios between 1.8 to 2 and for OD 260/230 ratio of 1.8 or greater. One microgram of total RNA was used, and three individual total RNA samples at the same time point were pooled as "single" sample in order to minimize both biologic variability and the number of microarrays necessary to generate informative data.[1] miRNA expression analyses were performed using an Affymetrix Gene-Chip miRNA Array (Affymetrix, Genisphere, FT30AFYB), which included poly(A) tailing with RNA samples, flash tag ligation, and hybridization. The chips were scanned, and the signal intensity was computed (GeneChip Command Console 1.1 software, Affymetrix, Santa Clara, California) according to the manufacturer's instructions and our previous report.[1] Transcript expression analyses were performed using an Affymetrix Expression Array (Affymetrix, Mouse Genome 430 2.0 Array), which involved cDNA synthesis, cRNA synthesis, amplification, purification, and hybridization. The microarray chips were scanned and the imaged data were processed using GeneChip Command Console 1.1 software (Molecular Devices, USA Affymetrix, Santa Clara, California) according to the manufacturer's instructions and our previous report.[1]

### 2.3 Data processing

The raw data were prepared using the 'affy' package in the Bioconductor project of the R software to obtain the expression values of the miRNA and mRNA probe set, including background correction, normalization, and summarization.[10-12]. Then, the self-written Perl language script program was used to convert the expression value of the mRNA probe set into the expression value of the gene (expressed by NCBI Entrez Gene ID, http://www.ncbi.nlm.nih.gov/gene). Finally, array were standardized, that is, the median expression value of all genes was subtracted from the expression value of each gene for each sample, so that the normalized miRNA and gene expression values were obtained. Only genes exhibiting an expression level fold change (FC) >1.5, or 1/FC<1.5 in the BPD group compared with that in the control group, were considered to reveal altered expression levels and were selected for further analysis.

### 2.4 GO and pathway enrichment analyses

Hyper-geometric distribution was used in this study for GO enrichment and KEGG pathway analyses.[13-16]. GO analysis included categories of cellular components (CC), biological processes (BP), and molecular functions (MF).[16] Herein, we focused on BP analysis. The pathway analysis is a functional analysis that maps genes to KEGG pathways. FDR q <0.01 was set as the cutoff point.

### 2.5 Combining expression profiles to predict credible miRNA-mRNA pairs

MiRanda (http://www.microrna.org),[17]Targetscans (http://www.targetscan.org),[18]and Pictar (http://pictar.mdc-berlin.de/cgi-bin/new_PicTar_mouse.cgi)[19,20] were used to predict candidate miRNA-mRNA pairs, and only union sets were examined further. Then, we selected more reliable miRNA-mRNA pairs by combining the gene expression profiles in our chip results; we focused on upregulated miRNA-downregulated mRNA pairs or downregulated miRNA-upregulated mRNA pairs. Finally, for each miRNA,

functional enrichment analysis of GO and KEGG pathways on its targets were performed to analyze the possible regulatory effects of miRNA.

### 2.6 Construction of a miRNA-mRNA regulatory network

IntAct (http://www.ebi.ac.uk/intact/),[21] and MIPS (http://mips.helmholtz-muenchen.de/proj/ppi/)[22]were used to collect empirically validated mouse protein-protein interaction (PPI) data, before they were merged into an integrated empirically validated PPI dataset. Meanwhile, TarBase (http://carolina.imis.athena-innovation.gr/diana_tools/web/index.php?r=tarbasev8/index)[23,24] was applied to collect empirically validated mouse miRNA-mRNA pair data. Thus, these verified data, together with our predicted candidate miRNA-mRNA pairs data from Section 2.5, were integrated into a global microRNA-mRNA regulatory network.[25,26] The visual representation of the network was drawn using Cytoscape.[27] The analysis pipeline for the complete analysis strategy was shown in Figure 1A.

### 2.7 Histological analysis

The right Llung tissue was fixed in 4% paraformaldehyde for 24 hovernight, and embedded with paraffin, and 5 μm sSections of 4 μm thickness were made under an ordinary Optical microscope and were cut. Sections were HE-stained stained as we previously described.[1]

### 2.8 Quantitative reverse transcription-PCR (qRT-PCR) validation and statistical analysis

Reverse transcription (RT) reactions and qRT-PCR were carried out as previously described. All miRNAs were normalized to u6, and all mRNAs were normalized to GAPDH. The relative expression levels of each gene were calculated using the $2^{-Ct}$ method as previously described.[1,28] All data were expressed as the mean± standard deviation. Student's t-test was used for comparisons between two groups. The statistical significance level was set at $p < 0.05$.

## RESULTS

### 3.1 Differentially expressed miRNAs and mRNAs

As we previously described, the BPD mouse model was established successfully after 21 days of hyperoxia exposure (Figure 1B). To validate microarray data, we randomly select 6 miRNAs[1]or 6 mRNAs to detect their expression levels by qRT-PCR (E-image 1), results revealed that these two methodologies had high internal consistency, and we can use these microarray data for further analysis.[1,28] According to the analysis pipeline (Figure 1A), we first analyzed differentially expressed miRNAs and mRNAs. Using a 1.5-fold difference in expression as a cutoff, a total of 192 differentially expressed miRNAs (74 downregulated and 118 upregulated) and 1225 differentially expressed mRNAs (479 downregulated and 746 upregulated) were identified between BPD mice and normoxia-control mice (E-Table 1 and E-Table 2, respectively). The top ten miRNAs and mRNAs were shown in E-Table 3 and E-Table 4, respectively.

### 3.2 GO and KEGG pathway enrichment of differentially expressed mRNAs

In total, 479 downregulated and 746 up-regulated mRNAs were analyzed with GO and KEGG pathway enrichment analysis. For downregulated genes, there were 35 GO enrichment processes with FDR<0.01. The top ten enriched BP were mainly related to immune and inflammation processes, such as, positive regulation of natural killer cell mediated cytotoxicity, and response to lipopolysaccharide (Figure 2A, E-Table 5). Furthermore, there were 7 enriched KEGG pathways with FDR<0.01, and these pathways were also largely related to immune and inflammation processes: cytokine-cytokine receptor interaction, natural killer cell mediated cytotoxicity, and Toll-like receptor signaling pathway (Figure 2B, E-Table 6). For the 746 upregulated genes, there were 62 GO enrichment processes with FDR<0.01. The top ten enriched BP were primarily related to heart muscle signal transduction, gluconeogenesis, and glycolysis processes (Figure 2C, E-Table 7). There were 9 enriched KEGG pathways with FDR<0.01 and these pathways were mainly related to olfactory transduction, ECM-receptor interaction, PPAR signaling pathway, cell Communication, gluconeogenesis and glycolysis pathways (Figure 2D, E-Table 8).

### 3.3 Candidate miRNA-mRNA pairs

A total of 787677 candidate miRNA-mRNA pairs were predicted using miRanda, Targetscans, and Pictar. Among these pairs, only the upregulated miRNA-downregulated mRNA pairs or downregulated miRNA-upregulated mRNA pairs were further selected based on the miRNA and mRNA expression profile data in Section 3.1 (E-Table 1, E-Table 2). Thus, a total of 3827 candidate miRNA-mRNA pairs were selected, and 83 miRNAs were involved. Among them, miRNA-374 had the largest number of targets (142 targets), and the gene 2810055g20 Rik was regulated by the most number of (29 miRNAs in total). The top 10 miRNA and mRNA were shown in Table 3.

Next, GO and KEGG function enrichment pathway analyses were performed on predicted targets of each differentially expressed miRNA. Some miRNAs-regulated targets were significantly enriched in immune regulation and inflammation-related functions, such as let-7f, miR-205, and miR-21 (Figure 3A-C). Correspondingly, the immune and inflammation-related genes were predicted to be downregulated, which was in agreement with the GO and KEGG function enrichment results for downregulated differentially expressed genes (Figure 2A, 2B, E-Table 5, E-Table 6). These miRNA-mRNA pairs are believed to play a role in biological and pathological mechanisms of BPD.

### 3.4 Immune and inflammation-related miRNA-mRNA regulatory network

The empirically validated mouse PPI interactions in the IntAct, MIPS, and MINT databases were collected, and a total of 4,853 PPI interactions were obtained after the union of these three sets. A total of 544 verified miRNA-mRNA pairs data were collected from TarBase. Furthermore, the 3827 miRNA-mRNA pairs obtained in Section 3.3 were integrated with the 4853 and 544 regulatory relationships to obtain a global miRNA-mRNA regulatory network (Figure 4A). Remarkably, among the differentially expressed genes, there were 117 genes for which the GO function or the GO function of the parent node was related to the immune system process. Then, based on the global miRNA-mRNA regulatory network, we further selected edges that contained at least one edge of these 117 genes from the global network (Figure 4A) to construct an immune and inflammation-related network. This network had 595 edges and was further divided into three subnetworks. The first subnetwork had 479 edges (Figure 4B), the second subnetwork had 115 edges (Figure 4C), and the third subnetwork had only 1 edge (Protein interaction between H2-Aa and H2 Ab1).

Interestingly, most miRNAs in the first subnetwork were upregulated, whereas most miRNAs in the second subnetwork were downregulated. Further enrichment analysis was performed on 106 genes in the first subnetwork. These 106 immune-related genes were largely involved in positively regulating the immune system: position regulation of NF kappaB transcription, position regulation of natural killer cell mediated cytotoxicity, position regulation of T cell promotion, and position regulation of interleukin-6 production (E-Table 9). There were 51 miRNAs involved in this subnetwork, including miR-21, let-7f, mir-431, and mir-205.

Functional enrichment analysis of 38 genes in the second subnetwork revealed that these 38 immune-related genes were involved in negatively regulating the immune system: negative regulation of cell promotion, negative regulation of plasma activation, negative regulation of response to stimulus, and negative regulation of immune system process (E-Table 10). However, these genes played a positive role in vascular proliferation and oxygen metabolism: positive regulation of angiogenesis and positive regulation of oxygen and reactive oxygen species metabolic process (E-Table 10). There were 30 miRNAs involved in this subnetwork, including mir-29b, mir-295 and mir-290-5p.

## DISCUSSION

Neonatal hyperoxia not only disrupts lung development, but also reprograms key immunoregulatory molecules in the lung.[29] However, at present, neonatal immunology is a poorly researched field, with only a handful of studies devoted to the pulmonary immune response;[3] thus, our report considerably expands knowledge in this field. In this study, we performed traditional bioinformatics methods to analyze the raw data and to identify miRNA-mRNA regulatory networks associated with immune and inflammation processes, which play key roles in the development of BPD.

The downregulated genes were mainly related with immune response and inflammatory processes, which emphasized their roles in BPD pathogenesis. There are studies indicate that the classic proinflammatory cytokines, including Il1α, Il8, Il1β and TNF-α are overexpressed during the saccular stage in neonates developing BPD, and their overexpression significantly disrupts lung development, both structurally and functionally.[3,4,8,30,31] While there are also reports demonstrate that some parameters of the early inflammatory response (neutrophils, cytokines such as Il1, TNF-α) may not be detectable after days to weeks of exposure to noxious stimuli; they have already initiated the signaling pathways of immune and inflammatory processes that can affect the BPD lung development.[30,32] The seemingly contradictory results may be due to the different stages of lung development or related with the complex inflammatory signal pathways during BPD pathogenesis. Therefore, a better understanding of the mechanisms underlying the dynamic immune and inflammatory responses during BPD development could reveal potential therapeutic targets to attenuate lung injury.

The upregulated genes were mainly related with ECM remodeling, and these data indicated that abnormal ECM remodeling was implicated in the pathogenesis of BPD, which is consistent with other reports.[33,34] Our previous studies also found that excessive production and accumulation of collagen appeared around the airways and blood vessels and in the alveolar regions of BPD mice, and a number of genes associated with ECM remodeling and fibrosis, such as fibronectin 1(FN1) and collagen 1α, were significantly dysregulated with the development of BPD,[33,34] these observations were also consistent with those of our current study. Moreover, these ECM components are believed to be involved in inflammation and immune-related signal pathways,[33-35] which supports the notion that the ECM process is central to the development of BPD.

Based on the miRNA-mRNA co-expression networks associated with immune and inflammation processes, we have found many important and interesting interactions between miRNAs and mRNAs. Some targeted genes are regulated by a single miRNA, whereas others can be regulated by multiple miRNAs which can interact with each other and form an interesting regulatory network. Of note, miR-205 was the most highly upregulated miRNA with 39 candidate targeted genes. These genes (such as H2-D1, Sh2d1a, Fcer2a, Lbp, Il18) are mostly enriched in immunity-related functions: positive regulation of lymphocyte mediated immunity, positive regulation of lymphocyte mediated immunity, positive regulation of immune response, positive regulation of lymphocyte mediated immunity, and induction of apoptosis. For example, Lbp has been investigated as a biomarker for inflammation.[36] It is an acute-phase protein essential for the response to bacterial lipopolysaccharides or endotoxins in gram-negative bacteria, and can also increase its expression in response to subclinical infections.[36] Taking miR-21 as another example, we found that it had 42 candidate targeted genes, and the functions of these genes were also related to immunity and inflammation, such as Il12a,[37] Cr2,[38]Lbp,[36] and Fasl.[39] Furthermore, these targeted genes may also be regulated by other miRNAs, such as miR-205 and miR-155,[18,40] or may be involved in other inflammatory pathways through signal interaction. Thus, these miRNAs and mRNAs construct regulatory networks associated with immune and inflammation processes by interacting with each other directly or indirectly. Further research will be needed to validate these miRNA-mRNA regulatory networks in detail, and we believe this will lead to additional significant findings.

In summary, this study characterized the miRNA and mRNA expression profiles of lungs under normoxic and hyperoxic conditions, providing insights into the immune and inflammatory responses to hyperoxia exposure during late BPD stages. Our findings further emphasize that the immune and inflammation processes play a significant role in BPD development and may provide relevant information for the development of new biomarkers and therapeutic targets not only to treat BPD, but also to facilitate normal adaptive immune responses, which will have broader implications in the management of premature infants.

## ACKNOWLEDGEMENT

This work was supported by the project supported by the National Natural Science Foundation of China (81270059); the Science and Technology Base and Talent Project of Guangxi Province (2019AD19003).

## AUTHOR CONTRIBUTIONS

XZ designed and supervised the study; ZW, SZ, LZ, JD, and BH performed the experiments and analysis work; XZ wrote the paper. All authors reviewed the final paper.

**Conflict of interest disclosure:** The authors declare no competing financial interests.

## REFERENCES

1. Zhang X, Peng W, Zhang S, et al. MicroRNA expression profile in hyperoxia-exposed newborn mice during the development of bronchopulmonary dysplasia. *Respir Care.*2011;56(7):1009-1015.

2. Villamor-Martinez E, Alvarez-Fuente M, Ghazi AMT, et al. Association of Chorioamnionitis With Bronchopulmonary Dysplasia Among Preterm Infants: A Systematic Review, Meta-analysis, and Metaregression.*JAMA Netw Open.* 2019;2(11):e1914611.

3. Nold MF, Mangan NE, Rudloff I, et al. Interleukin-1 receptor antagonist prevents murine bronchopulmonary dysplasia induced by perinatal inflammation and hyperoxia. *Proc Natl Acad Sci U S A.*2013;110(35):14384-14389.

4. Gronbach J, Shahzad T, Radajewski S, et al. The Potentials and Caveats of Mesenchymal Stromal Cell-Based Therapies in the Preterm Infant. *Stem Cells Int.* 2018;2018:9652897.

5. Ekiz HA, Ramstead AG, Lee SH, et al. T Cell-Expressed microRNA-155 Reduces Lifespan in a Mouse Model of Age-Related Chronic Inflammation.*J Immunol.* 2020;204(8):2064-2075.

6. Pham TT, Ban J, Lee K, et al. MicroRNA gga-miR-10a-mediated transcriptional regulation of the immune genes in necrotic enteritis afflicted chickens. *Dev Comp Immunol.* 2020;102:103472.

7. Coarfa C, Zhang Y, Maity S, et al. Sexual dimorphism of the pulmonary transcriptome in neonatal hyperoxic lung injury: identification of angiogenesis as a key pathway. *Am J Physiol Lung Cell Mol Physiol.* 2017;313(6):L991-L1005.

8. Butler B, De Dios R, Nguyen L, McKenna S, Ghosh S, Wright CJ. Developmentally Regulated Innate Immune NFkappaB Signaling Mediates IL-1alpha Expression in the Perinatal Murine Lung. *Front Immunol.*2019;10:1555.

9. Shivanna B, Maity S, Zhang S, et al. Gene Expression Profiling Identifies Cell Proliferation and Inflammation as the Predominant Pathways Regulated by Aryl Hydrocarbon Receptor in Primary Human Fetal Lung Cells Exposed to Hyperoxia. *Toxicol Sci.*2016;152(1):155-168.

10. Irizarry RA, Bolstad BM, Collin F, Cope LM, Hobbs B, Speed TP. Summaries of Affymetrix GeneChip probe level data. *Nucleic Acids Res.* 2003;31(4):e15.

11. Irizarry RA, Hobbs B, Collin F, et al. Exploration, normalization, and summaries of high density oligonucleotide array probe level data.*Biostatistics.* 2003;4(2):249-264.

12. Bolstad BM, Irizarry RA, Astrand M, Speed TP. A comparison of normalization methods for high density oligonucleotide array data based on variance and bias. *Bioinformatics.* 2003;19(2):185-193.

13. Harris MA, Clark J, Ireland A, et al. The Gene Ontology (GO) database and informatics resource. *Nucleic Acids Res.*2004;32(Database issue):D258-261.

14. Kanehisa M, Goto S. KEGG: kyoto encyclopedia of genes and genomes.*Nucleic Acids Res.* 2000;28(1):27-30.

15. Li Y, Li Q, Wang C, Li S, Yu L. Long Noncoding RNA Expression Profile in BV2 Microglial Cells Exposed to Lipopolysaccharide.*Biomed Res Int.* 2019;2019:5387407.

16. Wang W, Wang T, Wang Y, et al. Integration of Gene Expression Profile Data to Verify Hub Genes of Patients with Stanford A Aortic Dissection. *Biomed Res Int.* 2019;2019:3629751.

17. Betel D, Wilson M, Gabow A, Marks DS, Sander C. The microRNA.org resource: targets and expression. *Nucleic Acids Res.*2008;36(Database issue):D149-153.

18. Agarwal V, Bell GW, Nam JW, Bartel DP. Predicting effective microRNA target sites in mammalian mRNAs. *Elife.* 2015;4.

19. Krek A, Grun D, Poy MN, et al. Combinatorial microRNA target predictions. *Nat Genet.* 2005;37(5):495-500.

20. Jiang S, Fang X, Liu M, Ni Y, Ma W, Zhao R. MiR-20b Down-Regulates Intestinal Ferroportin Expression In Vitro and In Vivo. *Cells.*2019;8(10).

21. Kerrien S, Aranda B, Breuza L, et al. The IntAct molecular interaction database in 2012. *Nucleic Acids Res.* 2012;40(Database issue):D841-846.

22. Pagel P, Kovac S, Oesterheld M, et al. The MIPS mammalian protein-protein interaction database. *Bioinformatics.*2005;21(6):832-834.

23. Chou CH, Shrestha S, Yang CD, et al. miRTarBase update 2018: a resource for experimentally validated microRNA-target interactions.*Nucleic Acids Res.* 2018;46(D1):D296-D302.

24. Sethupathy P, Corda B, Hatzigeorgiou AG. TarBase: A comprehensive database of experimentally supported animal microRNA targets.*RNA.* 2006;12(2):192-197.

25. Nepusz, G.C.a.T. The igraph software package for complex network research. *InterJournal Complex Systems* . 2006; 1695.

26. Sacar Demirci MD, Yousef M, Allmer J. Computational Prediction of Functional MicroRNA-mRNA Interactions. *Methods Mol Biol.*2019;1912:175-196.

27. Shannon P, Markiel A, Ozier O, et al. Cytoscape: a software environment for integrated models of biomolecular interaction networks.*Genome Res.* 2003;13(11):2498-2504.

28. Zhang X, Liu S, Hu T, Liu S, He Y, Sun S. Up-regulated microRNA-143 transcribed by nuclear factor kappa B enhances hepatocarcinoma metastasis by repressing fibronectin expression. *Hepatology.*2009;50(2):490-499.

29. Kumar VHS, Wang H, Nielsen L. Adaptive immune responses are altered in adult mice following neonatal hyperoxia. *Physiol Rep.*2018;6(2).

30. Balany J, Bhandari V. Understanding the Impact of Infection, Inflammation, and Their Persistence in the Pathogenesis of Bronchopulmonary Dysplasia. *Front Med (Lausanne).* 2015;2:90.

31. Kasat K, Patel H, Predtechenska O, Vancurova I, Davidson D. Anti-inflammatory actions of endogenous and exogenous interleukin-10 versus glucocorticoids on macrophage functions of the newly born.*J Perinatol.* 2014;34(5):380-385.

32. Kramer BW, Kallapur S, Newnham J, Jobe AH. Prenatal inflammation and lung development. *Semin Fetal Neonatal Med.* 2009;14(1):2-7.

33. Zhang X, Xu J, Wang J, et al. Reduction of microRNA-206 contributes to the development of bronchopulmonary dysplasia through up-regulation of fibronectin 1. *PLoS One.* 2013;8(9):e74750.

34. Zhang X, Wang H, Shi Y, et al. Role of bone marrow-derived mesenchymal stem cells in the prevention of hyperoxia-induced lung injury in newborn mice. *Cell Biol Int.* 2012;36(6):589-594.

35. Fujiu K, Manabe I, Nagai R. Renal collecting duct epithelial cells regulate inflammation in tubulointerstitial damage in mice. *J Clin Invest.* 2011;121(9):3425-3441.

36. Mengel A, Ulm L, Hotter B, et al. Biomarkers of immune capacity, infection and inflammation are associated with poor outcome and mortality after stroke - the PREDICT study. *BMC Neurol.*2019;19(1):148.

37. Liaskou E, Patel SR, Webb G, et al. Increased sensitivity of Treg cells from patients with PBC to low dose IL-12 drives their differentiation into IFN-gamma secreting cells. *J Autoimmun.*2018;94:143-155.

38. Preisker S, Brethack AK, Bokemeyer A, Bettenworth D, Sina C, Derer S. Crohn's Disease Patients in Remission Display an Enhanced Intestinal IgM(+) B Cell Count in Concert with a Strong Activation of the Intestinal Complement System. *Cells.* 2019;8(1).

39. Yu T, Liu D, Zhang T, Zhou Y, Shi S, Yang R. Inhibition of Tet1- and Tet2-mediated DNA demethylation promotes immunomodulation of periodontal ligament stem cells. *Cell Death Dis.* 2019;10(10):780.

40. Ma CJ, Liu X, Che L, Liu ZH, Samartzis D, Wang HQ. Stem Cell Therapies for Intervertebral Disc Degeneration: Immune Privilege Reinforcement by Fas/FasL Regulating Machinery. *Curr Stem Cell Res Ther.* 2015;10(4):285-295.

## FIGURE LEGENDS

FIGURE 1. **Analysis pipeline (A) for hyperoxia-exposed neonatal mice model (B).** (B) showed lung structure was markedly abnormal, with enlarged air spaces and simplified structure, in neonatal mice exposed to hyperoxia from P7 to P21, compared with air controls. Bars represent m.

FIGURE 2. **Enriched GO terms analysis and KEGG pathway analysis for differentially expressed mRNAs.** (A) Top 10 significantly enriched GO terms of downregulated mRNA-BP. (B) Top 7 significantly pathways of downregulated mRNA. (C) Top 10 significantly enriched GO terms of upregulated mRNA-BP. (D) Top 9 significantly pathways of downregulated mRNA.

FIGURE 3. **Enriched GO terms analysis for predicted targets of each differentially expressed miRNA.** (A) Left: the enriched GO BP of let target genes; Right: the visualization of let regulated targets. (B) Left: the enriched GO BP of miR-21 target genes; Right: the visualization of miR-21 regulated targets. (C) Left: the enriched GO BP of miR-205 target genes; Right: the visualization of miR-205 regulated targets. (a-c) The depth of color represented the value of (FC-1) if FC larger than 1, otherwise represented the value of (-1/FC+1). Red meant upregulation, green meant downregulation while white meant no change.

FIGURE 4. **Immune and inflammation-related miRNA-mRNA regulatory network.** (A) Visualization of the global miRNA-mRNA regulated network. Red node represented gene, green node represented miRNA. Grey edge represented predicted miRNA-mRNA pairs, yellow edge represented empirically validated miRNA-mRNA pairs while blue edge represented PPI. (B) The visualization of the first immune related subnetwork. (C) The visualization of the second immune related subnetwork. (b-c) The rectangle represented miRNA while circle represented gene. The depth of color represented the value of (FC-1) if FC larger than 1, otherwise represented the value of (-1/FC+1). Red meant upregulation, green meant downregulation while white meant no change. Grey node represent the gene whose expression can not be detected in our profiles. Red edge represented the empirically validated miRNA-mRNA pairs, grey edge represented our predicted miRNA-mRNA pairs while blue edge represented PPI.

E-image 1. **Correlation of 6 mRNAs levels between mRNA microarray and real-time PCR analyses.** (A) The expression levels were independently assessed by microarray and real-time PCR, and (B) the results in both methodologies demonstrated very high internal consistency with a correlation coefficient (R2) of 0.904, and p value $< 0.01$ (Pearson).

### Hosted file

`Table 1.docx` available at https://authorea.com/users/357208/articles/479859-integrated-microrna-mrna-analyses-of-distinct-expression-profiles-in-hyperoxia-induced-bronchopulmonary-dysplasia-in-neonatal-mice

Fig. 1.

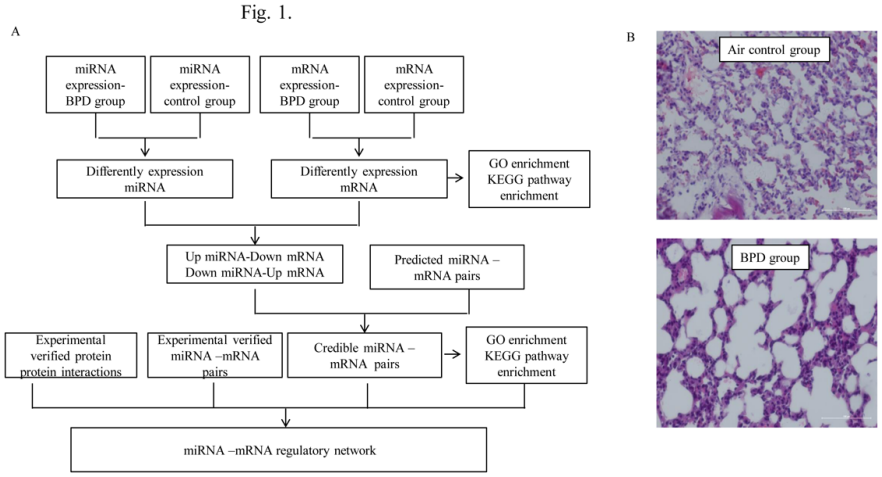


Fig. 2.

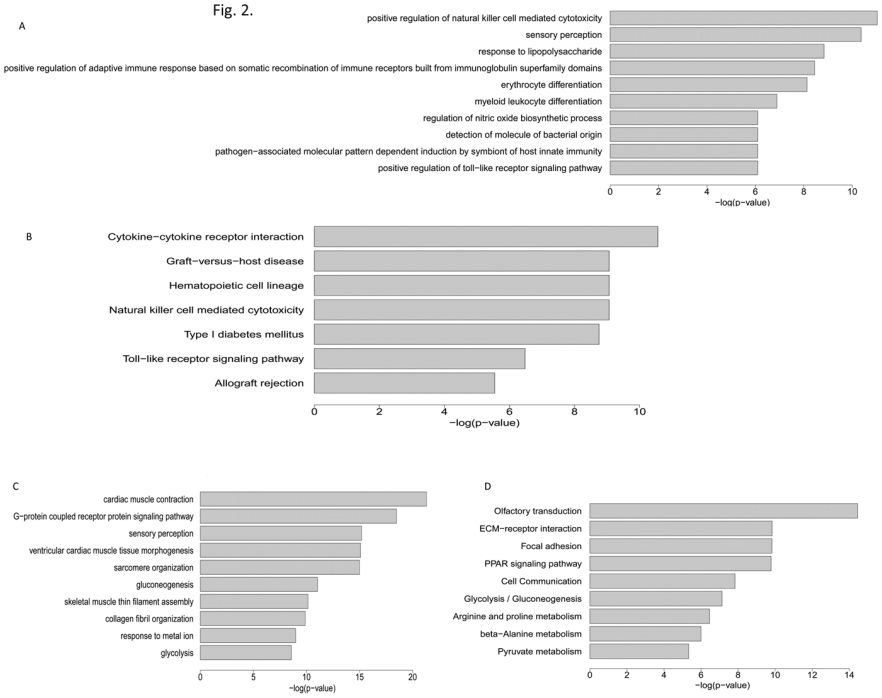

Fig.3.

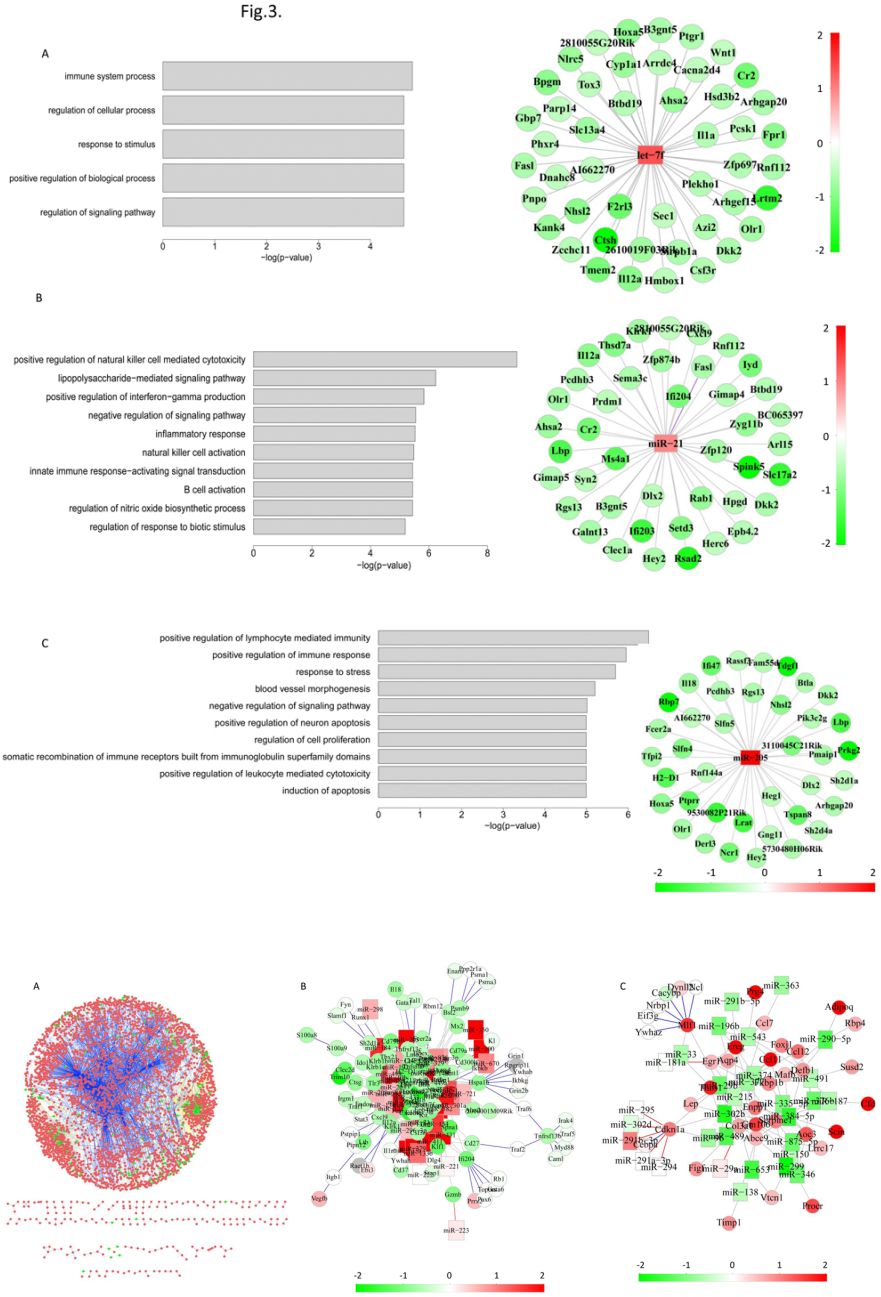

Fig. 1.

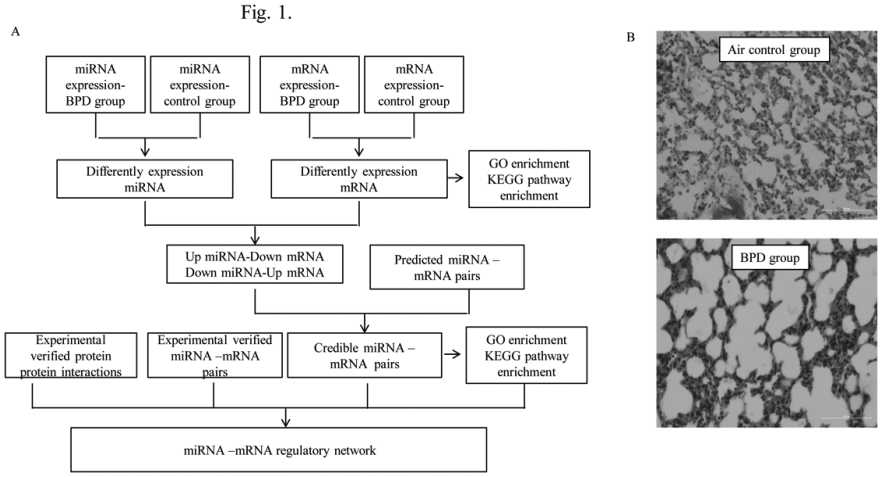


Fig.3.